AL-ZAHRAA UNIVERSITY JOURNAL
Health and Medical Science

Al-Zahraa Journal for Health and Medical Sciences 2025; 3:76-90 Vol. 3, No.2, 2025
www.zjhms.alzahraa.edu.iq

Microwave-Induced Green Synthesis of Meso-structured MCM-41 in CTAB template and using in Photodecolorization of Eosin Yellow Dye

Rawaa A. Alattar[1], Hayder Hamied Mihsen[1] and Luma Majeed Ahmed[2,1]

[1] Department of Chemistry, College of Science, University of Kerbala, Karbala, Iraq.
[2]Al-Zahraa Center for Medical and Pharmaceutical Research Sciences (ZCMRS), Al-Zahraa University for Women, Karbala, Iraq.
* rawaa.a@uokerbala.edu.iq

Received: 19 June 2025, Accepted: 28 June. 2025. Published: 30 June. 2025

ABSTRACT

One of the most prevalent agricultural wastes is rice husk (RH). RH reacts with sodium hydroxide solution to produce sodium silicate, which can be converted to Mobil Composition of Matter No. 41 (MCM-41) via an eco-friendly route. MCM-41 was successfully synthesized in the form of a meso-porous silica via an enhanced microwave technique at 100 °C for 20 min. The silanol group in MCM-41 was identified as a sharp peak around 3510 cm^{-1} in the FT-IR spectrum. A nanoscale hexagonal structure of mesoporous silica was determined via XRD analysis and TEM analysis. The surface area of MCM-41 is high at 1024.9 m^2/g, with an average pore diameter in the meso-porous material of 2.7314 nm. FESEM images show that MCM-41 particles are smooth, forming spherical agglomerations. According to EDX analysis, Si and O are present in a sample that appears otherwise essentially free of impurities. The Photo-decolorization kinetic of 5 mg/L Eosin yellow dye on the MCM-41 surface were found to be pseudo-First order in nature at optimum physical conditions of pH 8, 25 °C, MCM-41 dosage of 0.05 g and an irradiation period of 80 minutes. Furthermore, The thermodynamic functions (ΔH#, ΔS#, and ΔG#) for this photoreaction demonstrated the reaction is exothermic, not spontaneous, and random less.

Keywords: Rice Husks, MCM-41, Eosin yellow dye, Removal treatment, Photo-decolorization, Thermodynamics.

IRAQI Academic Scientific Journals

Introduction

In the world, rice is the second most popular cereal [1].With an annual production of over 715 million tons, rice is a staple crop that is currently grown in more than 100 countries and consumed globally [2]. Numerous studies have demonstrated that fly ash and rice husk, which are waste products from burning coal and milling rice, contain around 95% silica and are therefore suitable sources of mesoporous silica, such as MCM-41[3]. RH, one of the industry's byproducts, is an inexpensive and accessible source of silicates and silica[4]. Due to its large specific surface areas, uniform pore volumes, and hydroxyl groups that can interact with other chemicals, mesoporous silica (MCM-41, mobile composition of material no. 41) is a porous material that is frequently used as an adsorbent[5]. Green chemistry in nanotechnology is concerned with the production, synthesis, application, and disposal of nanomaterials to solve problems related to the environment and public health[6]. To lower total energy consumption, microwave technology is used as a backup heat source during the MCM-41 production process[7]a. Rapid nucleation during crystallization may be made possible by the quick heating, homogenization, and high penetration of microwave synthesis, which can also improve the interaction between surfactants and silicon species. Since microwave radiation is a more efficient technique than conventional heating, it is frequently employed in chemical processing[7]. In earlier research, it was discovered that sorbents made with microwave assistance performed better than those made using reflux heating [8]. Industries all over the world have put various strategies into place to clean wastewater before releasing it into the environment, and a variety of cutting-edge concepts and technologies are currently quickly replacing the related traditional methods[9]. Textiles and numerous other sectors use dyes, a significant class of synthetic organic compounds. Because of this, they are now frequently emitted industrial pollutants during the fiber synthesis and, subsequently, the dyeing process[10]. Since adsorption is a straightforward and effective method, it has been used extensively for many years to remove coloring from aqueous solutions. Eosin Yellow (2-(2,4,5,6-Tetrabromo-6-oxido-3-oxido-3H xanthenes-9-yl) benzoate disodium), an acidic natural dye that is very water soluble, is one of the most dangerous dyes in aqueous solutions. It is frequently used in gram staining to distinguish between various bacterial species due to its red color and significant absorption by red blood cells. [11]. The current study aims to create a quick and affordable technique for photodecolorizing Eosin Yellow dye using MCM-41. MCM-41 nanomaterial is synthesized from rice husk (RH) via microwave-assisted green synthesis. Due to its high surface

area compared to other similar substances, 1049.2 m^2 g^{-1}, it has been applied herein in the Photo-decolorization of Eosin yellow dye. The optimal parameters for this process, initial pH, adsorbent dose, and temperature, have been studied and determined; based on these findings, thermodynamic parameters for the Photo-decolorization process have been established.

EXPERMINTEL

CHEMICAL MATERIALS

The local rice manufacturing factory in the city of Abbasiya, Najaf Governorate, provided the rice husks for collection. Cetyltrimethylammonium bromide (CTABr, Merck, 98 %) was used to facilitate the synthesis of MCM-41. Absolute ethanol (Fluka, >99 %), nitric acid (BDH, 65 %), sodium hydroxide (Merck, 99 %), acetic acid (BDH, 99.5 %), acetone (Romal, 99.7 %), and Eosin yellow dye ($C_{20}H_6Br_4Na_2O_5$) were purchased from BDH. All chemicals were used without further purification.

Synthesis of sodium silicate solution from rice husk

Next washing the RH with water to clear it of any grime, mud, or solid debris, it was then allowed to dry. 30 g of dried RH was placed in a plastic container and 500 mL 1.0 M nitric acid added, and the resultant mix gone for 24 hours at room temperature. After rinsing the RH with deionized water to neutralize the acid (pH 6-7), it was dried overnight at 110 ^oC in an oven. The RH was then shaken for 24 hours at room temperature in 200 mL, 1 M NaOH. A black filtrate (sodium silicate) was obtained by filtering this mixture, which was then stored in a covered plastic container. Using RH, a sodium silicate solution could thus be made up [12].

Synthesis of MCM-41

CTABr was utilized as a template to synthesize MCM-41. After dissolving 1 g of CTABr in 100 mL DI water while stirring at 25 ^oC, 100 mL sodium silicate solution from RH was added dropwise to create a surfactant-silica combination. The mix was moved at 25 ^oC for 6 hours after the pH was adjusted to 10 using 1 M acetic acid. The surfactant-silica gel mixture was microwave-heated for 20 minutes at 200 W at 100 ^oC and then allowed to age for 24 hours. Finally, the hard produce was filtrated, washed with DI water, then calcinated in a furnace at 500 ^oC for 5 hours. MCM-41 was obtained as a white solid powder. The steps to the production of MCM-41 using the microwave technique are illustrated in Fig. 1.

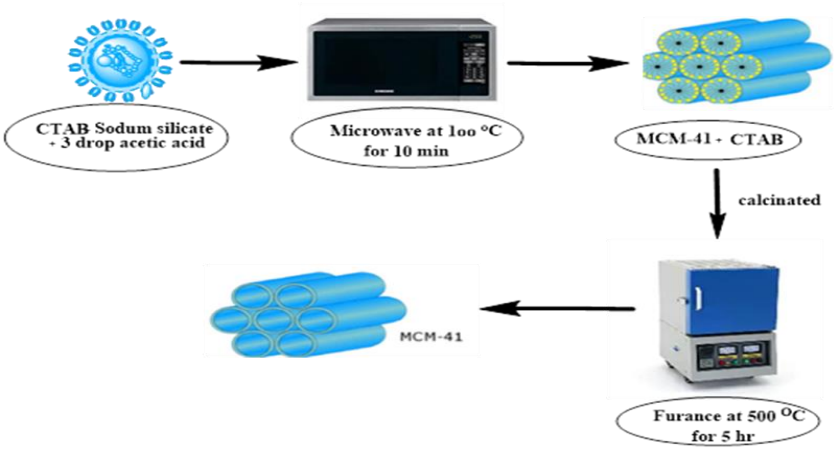

Fig. 1 Schematic diagram of MCM-41 production using the microwave synthesis technique.

Sample Characterization

Using specimens formed in KBr discs, FT-IR spectra were captured on a Shimadzu 8400 spectrophotometer in the 4000–400 cm^{-1} range. A Shimadzu X-ray diffractometer was used to record the X-ray diffraction (XRD) patterns, whilst a BET BELSORP MINI II apparatus was used to perform the nitrogen adsorption/desorption analysis. Thermogravimetric analysis (TGA/DTA) was performed on an SDT Q600 V20.9 Build 20, Atomic force microscopy (AFM) Beam Gostar Taban Lab-Iran, FESEM MIRA III (TESCAN) Beam Gostar Taban Lab-Iran and High Resolution Transmission Electron Microscopy (HRTEM), to 20 nm.

Photodecolorization of Eosin Yellow Dye using MCM-41 NPs

Using a homemade photoreactor, numerous tests were conducted to determine the ideal conditions for photo reactions. [13]. The reactor's body is prepared from a wooden box to avoid harmful light, which contains an inside 125-watt mercury lamp (UV-A), Pyrex glass beaker (500 mL), magnetic stirrer, Teflon bar, and fun. The light source of this reactor was horizontally located above the solution in a glass container. At different temperatures (10, 15, 20 and 25 °C), with range pH (3-9), and dose (0.05-0.3 g) of studied photocatalysts was dispersed in 5 ppm of 100 mL Eosin yellow dye solution. The subsequent suspension solution was moved for 30 minutes to establish an equilibrium state. The UV light was applied on the suspension after the initial step (adsorption). From the photoreaction, the following equations were used to determine the photodecolorization efficiency (Edecol%) and the apparent rate constant (kapp.) [14][15].

$$ln\left[\frac{C_o}{C_t}\right] = K_{app}\,.\,t \qquad (1)$$

$$\%E_{decol.} = \left[\frac{C_o - C_t}{C_o}\right] \times 100 \quad (2)$$

whereas: C_o and C_t are an initial concentration of dye in dark reaction and a concentration of the same dye at t time of irradiation.

RESULT AND DISSCUSSION

FTIR Spectroscopy Analysis

The FT-IR spectrum of MCM-41 is presented in Fig. 2. The -OH of the silanol group (Si–OH) and the hydroxyl groups in adsorbed water particles on the surface of the silica were identified as having a broad absorption band at about 3510 cm^{-1}[12]. The O-H bending vibration for silanol groups was identified as the band at 1666 cm^{-1}[16]. Additionally, bands at 825 and 1130 cm^{-1} in the FT-IR spectrum were identified as corresponding to the symmetric and antisymmetric stretching of Si–O–Si bonds. These results are in good agreement with earlier studies[17].

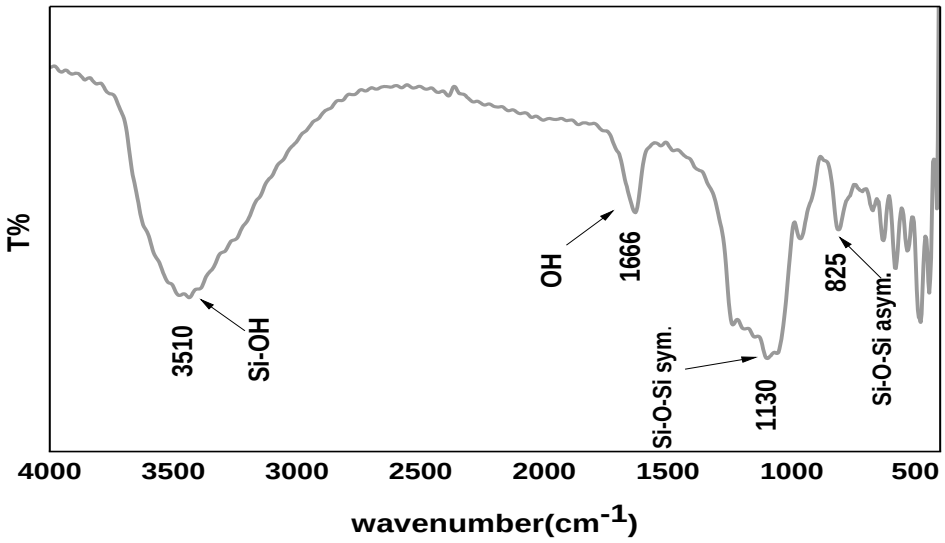

Fig. 2 The FT-IR spectrum of MCM-41.

X-Ray Diffraction Pattern

The small angle XRD spectrum for MCM-41 is presented in Fig. 3. The anticipated diffraction peaks of MCM-41 are situated at roughly 2.65°, 4.55°, 5.35°, and 6.15°, respectively, and represent the (100), (110), (200), and (210) planes. The peaks at these locations reflect the hexagonal porous structure that characterizes MCM-41[18]. Fig. 4 displays the high angle XRD study. The MCM-41's amorphous structure itself produces a broad feature at 2θ = 22°[19]. The mean crystal size before

MCM-41 adsorption was 1.266 nm, according to low angle XRD data and the Deby-Scherrer formula. This indicates that the Eosin yellow dye adsorbed on the surface will bind to the active sites and coat the MCM-41 surface, increasing the particle size.

$$D = \frac{k\lambda}{\beta cos\theta} \qquad (1)$$

Here, λ is the wavelength of the X-ray (1.5406 Å for Cu Kα), and β is the peak's full width half maximum (FWHM), D is the crystal size, and θ is the Bragg angle. For MCM-41, three distinctive diffraction peaks (100), (110), and (200) are visible, indicating strong crystallinity as a result of the pores' hexagonal hope.

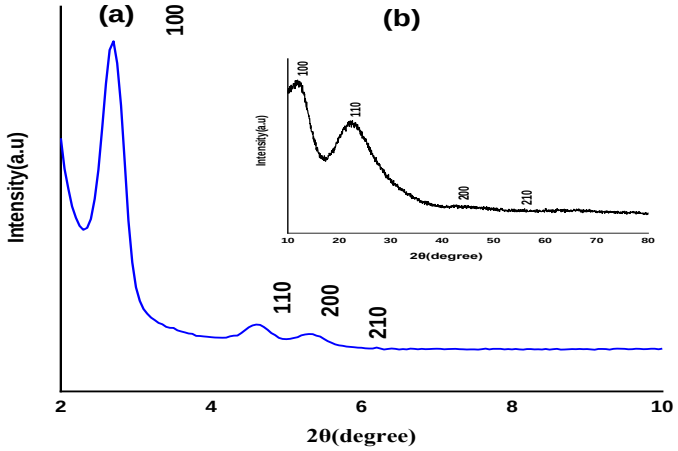

Fig.3(a) The low angle XRD spectrum and (b) The high angle XRD spectrum of MCM-41.

N_2 Adsorption-Desorption Analysis

Figure 5 shows the N_2 adsorption/desorption isotherm curves that were acquired for MCM-41 nanoparticles. A type IV isotherm, which is common for mesoporous solids, was displayed by MCM-41[19]. The exhibited curves exhibit hysteresis loops of the H4 type, which are more commonly found in synthetic solids, such as artificially agglomerated particles having spheroidal forms or other interior cylindrical channels. These nanoparticles appear to have a mesoporous structure based on their measured surface area, average pore diameter, and pore volume, which were 1049.2 m^2/g, 2.7314 nm, and 0.6999 cm^3/g, respectively. Because of their porosity, reactants may more easily reach the active sites on the nanoparticles' surface, making them suitable for a range of applications such as impurity removal, adsorption, and catalysis[20].

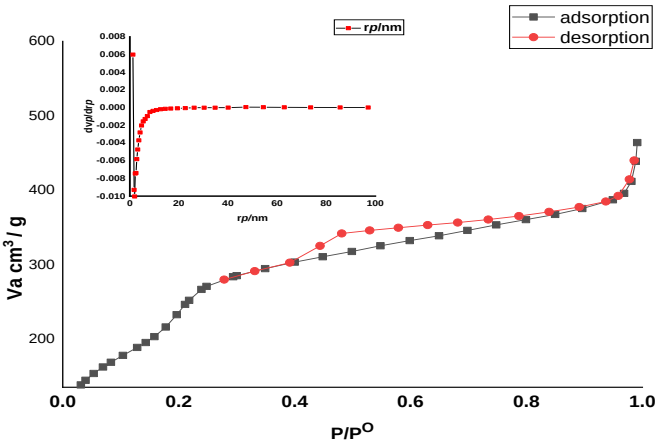

Fig. 4 The N_2 adsorption-desorption isotherm and pore size distribution of MCM-41.

FESEM and EDX Analysis .

The size and morphology of the produced species were tracked using FESEM [21]. This method creates high-resolution, high-magnification images by using electron microscopy to examine subatomic particles and sample composition. Fig. 5 displays MCM-41's FESEM-EDX and the results got from EDX analysis for MCM-41. The pictures demonstrate that MCM-41 particles form spherical agglomerations and are smooth [22].

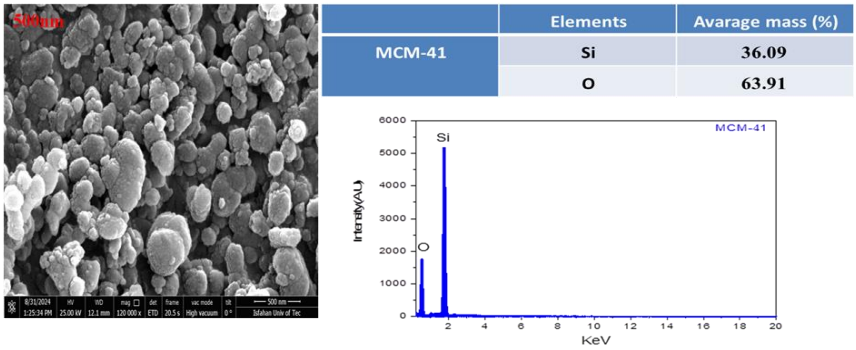

Fig.5 FESEM-EDX and results from EDX analysis for MCM-41.

An elemental analysis method related to electron microscopy, energy dispersive X-ray (EDX) spectroscopy relies on the generation of distinctive X-rays that indicate the presence of specific elements in the samples[21]. The most prevalent element in the sample, according to the EDX chemical analysis, is silicon (Si).

TEM Analysis

An additional indication that MCM-41, as made by the microwave process, has a mesoporous structure is the mesoporous channel section, which appears as a regular hexagon in the channel

direction [23]. The thickness of the pore wall was estimated to be around 2.1 nm using the TEM images (Fig. 6).

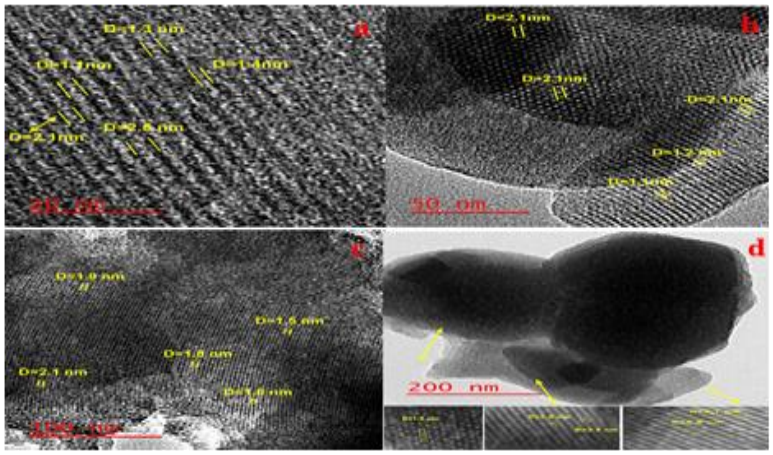

Fig. 6 TEM imagery of MCM-41 on scales of (a) 20 nm, (b) 50 nm, (c) 100 nm, and (d) 200 nm.

Photodecolorization of Eosin Yellow Dye using MCM-41 as an Adsorption Surface

The solution was prepared by adding a suitable weight (0.05g) of studied photocatalysts to 5 ppm of Eosin yellow dye solution. The subsequent suspension solution was moved for 30 minutes to found an equilibrium state. The UV light was applied on the suspension after the initial step (adsorption). About 3 mL of solution were collected at various intervals time ranged (0, 10, 20,30,40,50,60,70 and 80 min) at 25 ^{o}C and pH=8 .The produced filters were twice times separated by a centrifuge, and the absorption of the produced filters was measured at λ_{max} = 510 nm. Using UV-visible spectroscopy[24]. The Langmuir-Hinshelwood (L-H) model states that pseudo first-order kinetics govern the rate of reaction[19], as shown in Fig.7.

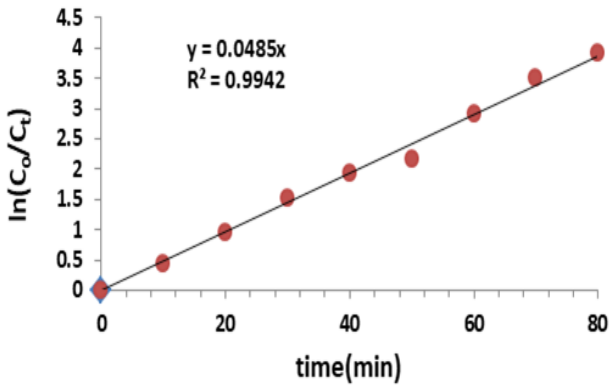

Fig.7: First-order model for photodecolorization of Eosin yellow dye on MCM-41 surface, (conditions: pH 8; dosage = 0.05 g; time=(0-80) min, concentration of dye 5 mg/L and temperature = 25 ^{o}C).

Effect of MCM-41 dose on photodecolorization of Eosin yellow dye.

The effect of MCM-41 doses in the various weights ranged (0.05- 0.30 g) is depicted in Fig.8. The decolorization efficiency was found to drop from 96.045% with 0.05 g of MCM-41 to 92.33% with 0.3 g. These findings imply that lowering the dosage of MCM-41 results in fewer active sites on the photocatalyst surface, which are necessary for activation [25].

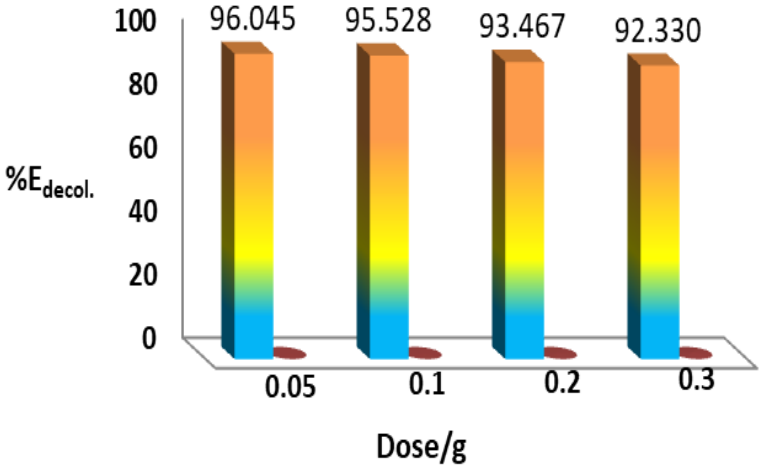

Fig.8: % $E_{decol.}$ of Eosin yellow dye as a function of MCM-41 dose, conditions: pH 8; dosage = (0.05-0.3)g; time=80 min, concentration of dye 5 mg/L and temperature = 25 ^{o}C).

Effect of Initial pH of Eosin yellow dye Solution.

The percentage of decolorization increases as pH rises from 3 to 9, as shown in Fig. 9. There are two possible explanations for these outcomes: the dye's characteristics and the photocatalyst surface's characteristics[26]. In the acidic medium's the decolorization efficiency values are good. This outcome is consistent with the literature, which shows that MCM-41's zero electrical point is 2.28[27]. The maximum decolorization efficiency surpasses 97.412% at pH 9. Furthermore, the dye's hue changes at pH values higher than 9, which results in limited efficiency[28]. This behavior suggests that in a basic media , MCM-41's surface charge turns negative, increasing the electrostatic repulsion of the anionic Eosin yellow dye[29].

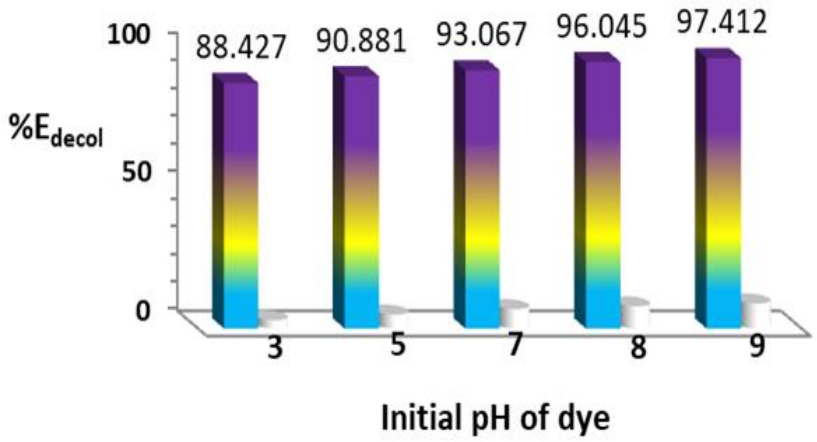

Fig.9: % E_{decol} of Eosin yellow dye at different initial pH (3-9) and dosage = 0.05 g; time=80 min, concentration of dye 5 mg/L and temperature 25 ^{o}C).

Decolorization of dye below numerous temperature

Figure 10 shows the removal percentage of dye (5 mg/L) by 0.05 g MCM-41 surfaces at pH=9 under UV radiation and at various temperatures (10, 15, 20, and 25 ^{o}C). The maximum decolorization percentage was 96.045% at temperature 25 ^{o}C following 30 minutes of illumination. The activation energy (Ea) from the impact temperature range (288-303) K[30] and the Arrhenius equation was used to measure the thermodynamic function for the active case in the photo process ($\Delta H^{\#}$, $\Delta S^{\#}$, and $\Delta G^{\#}$)[31], the Eyring-Polanyi equation, and the Gibbs equation[32]. These results are shown in Fig.11(a,b) and table 1.

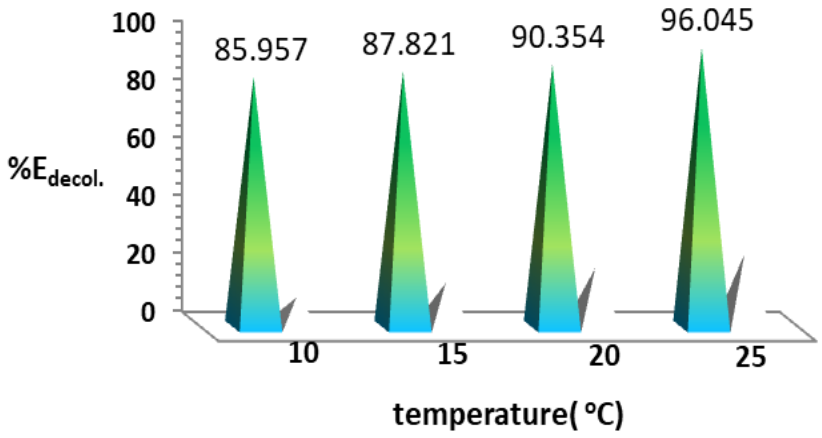

Fig.10: $\%E_{decol.}$ of Eosin yellow dye at different temperature,(conditions: pH 9; dosage = 0.05 g; time=80 min, concentration of dye 5 mg/L and temperature = (10-25) ^{o}C).

Table 1: Thermodynamic effects and activation energy values of the parameters for the photodecolorization of eosin yellow dye.

Ea kJ mol^{-1}	$\Delta H^{\#}$ kJ mol^{-1}	$\Delta S^{\#}$ J mol^{-1} K^{-1}	$\Delta G^{\#}$ kJ mol^{-1}
41.816	-2.413	-0.221	63.721

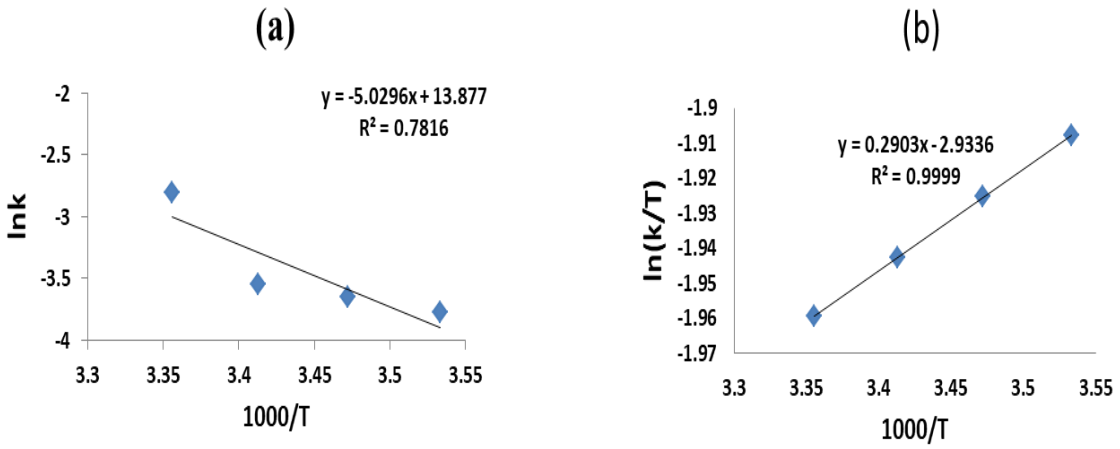

Fig.11: (a) Arrhenius equation plot and (b) Eyring equation plot for photodecolorization of Eosin yellow dye at different temperature

Eosin yellow dye decolorization was accelerated by UV light-induced temperature increases, as shown in Fig.11 (a,b) and Table 1. Exothermic and nonspontaneous, the photoreaction of Eosin yellow dye decolorization is indicated by the negative $\Delta H^{\#}$ and the positive $\Delta G^{\#}$[14] The less random stage of photoreaction is denoted by a negative $\Delta S^{\#}$. The low activation energy value suggests a quick photoreaction of decolorization [33]. These findings were thought to be in good agreement with earlier published reference [34].

Conclusion

This research considers the synthesis, investigation, and application of MCM-41 nanoparticles for the active deletion of Eosin yellow dye from aqueous solution. In this study, MCM-41 nanoparticles were successfully synthesized from rice husk with the aid of CTABr via a green method (microwave technique) at 100 °C for 20 min. Thorough analysis of the MCM-41 nanoparticles was achieved using several techniques, namely FTIR, XRD, BET, TGA, FESEM, EDX and HR-TEM. The silanol group in MCM-41 (a broad peak) and the symmetric and antisymmetric stretching of

Si–O–Si bonds were identified via FT-IR analysis. A nanosized hexagonal structure of mesoporous silica was demonstrated via XRD analysis. The mean crystal size prior to adsorption by MCM-41 was determined to be less than the mean crystal size post-adsorption, indicating that the Eosin yellow dye will bind to the active sites on the surface of MCM-41 and coat it, thus increasing the particle size. Furthermore, the nitrogen adsorption-desorption analysis (BET) established the measured surface area, average pore diameter, and pore volume, suggesting these nanoparticles have a mesoporous structure and high surface area, demonstrating their efficient adsorption by MCM-41. FESEM was used to monitor the size and morphology of the MCM-41 prepared. The images show MCM-41 particles are smooth and form spherical agglomerations. According to EDX analysis, Si and O were present in the sample without impurities. The TEM analysis implied that MCM-41 has a well-ordered hexagonal arrangement and was used to determine the average particle size, which was found to be 2.1 nm as quantum dot nanomaterial. The photodecolorization of Eosin yellow dye onto MCM-41 surface was found to obey a pseudo-First order model under optimum conditions. The thermodynamic function $\Delta H^{\#}$, $\Delta S^{\#}$, and $\Delta G^{\#}$ were calculated and proved, this photoreaction is nonspontaneous, random less and exothermic in nature.

Acknowledgments

The authors would like to thank the University of Kerbala, College of Science, Department of Chemistry, for their support in this study, the practical part of which was undertaken in their chemistry laboratory.

Author contributions The manuscript was prepared with contributions from all authors. All authors have approved the final version of the manuscript.

Funding This project did not receive any funding.

Data availability No datasets were generated or analyzed during the current study.

Declarations

Ethical approval Not applicable.

Competing interests The authors declare no competing interests.

References

[1] Mohsin, A. D. and Mihsen, H. H., 2020. “Uptake of metal ions (Co (II) and Ni (II)) by silica-salicylaldehyde derived from rice husks,” *J. Inorg. Organomet. Polym. Mater.*, vol. 30, pp. 2172–

2181. https://doi.org/10.1007/s10904-019-01379-7

[2] Requena, R., Jimenez-Quero, A., Vargas, M., Moriana, R., Chiralt, A. and Vilaplana, F., 2019. "Integral fractionation of rice husks into bioactive arabinoxylans, cellulose nanocrystals, and silica particles". *ACS Sustainable Chemistry & Engineering*, *7*(6), pp.6275-6286. https://doi.org/10.1021/acssuschemeng.8b06692

[3] Bhagiyalakshmi, M., Yun, L.J., Anuradha, R. and Jang, H.T., 2010. "Synthesis of chloropropylamine grafted mesoporous MCM-41, MCM-48 and SBA-15 from rice husk ash: their application to CO_2 chemisorption". *Journal of Porous Materials*, *17*, pp.475-484. https://doi.org/10.1007/s10934-009-9310-7475–484.

[4] Al Soubaihi, R.M., Saoud, K.M., Ye, F., Myint, M.T.Z., Saeed, S. and Dutta, J., 2020. "Synthesis of hierarchically porous silica aerogel supported Palladium catalyst for low-temperature CO oxidation under ignition/extinction conditions". *Microporous and Mesoporous Materials*, *292*, p.109758. https://doi.org/10.1016/j.micromeso.2019.109758

[5] Zasypalov, G., Vutolkina, A., Pimerzin, A., Klimovsky, V., Abramov, E. and Glotov, A., 2025. "The beneficial effect of halloysite nanotubes as a matrix preventing the break of ordered mesoporous silica structure under microwave-assisted metal deposition". Applied Clay Science, 265, p.107686.https://doi.org/10.1016/j.clay.2024.107686

[6] Ni, Z., Hojo, H. and Einaga, H., 2025. "Microwave-Assisted Heating for Dehydration of Ethanol to Ethylene Using HPW/SBA-15". *Industrial & Engineering Chemistry Research*.. https://doi.org/10.1021/acs.iecr.4c04420

[7] Tiwari, S. and Talreja, S., 2022. "Green chemistry and microwave irradiation technique: a review". *Green Chemistry*, *11*, p.15. DOI: 10.9734/JPRI/2022/v34i39A36240

[8] Ji, T., Zhai, H., Wang, C., Culp, J., Marin, C.M., Paudel, H.P., Wilfong, W.C., Duan, Y., Xia, R., Jiao, F. and Kail, B., 2022. "Microwave-accelerated regeneration of a non-aqueous slurry for energy-efficient carbon sequestration". *Materials Today Sustainability*, *19*, p.100168. https://doi.org/10.1016/j.mtsust.2022.100168

[9] Bora, T. and Dutta, J., 2014. "Applications of nanotechnology in wastewater treatment—a review". *Journal of nanoscience and nanotechnology*, *14*(1), pp.613-626. https://doi.org/10.1166/jnn.2014.8898

[10] Khattab, T.A., Abdelrahman, M.S. and Rehan, M., 2020. "Textile dyeing industry: environmental impacts and remediation". *Environmental Science and Pollution Research*, *27*(4), pp.3803-3818.. https://doi.org/10.1007/s11356-019-07137-z

[11] Costa, R.G., Esteves, W.T.C. and da Rocha Nogueira, J.M., 2024. "Main classical staining methods in

bacteriology: applications, techniques, principles, and limitations". *RBAC*, *56*(3), pp.197-210.

[12] Kamari, S. and Ghorbani, F., 2021. "Extraction of highly pure silica from rice husk as an agricultural by-product and its application in the production of magnetic mesoporous silica MCM–41". *Biomass Conversion and Biorefinery*, *11*(6), pp.3001-3009. https://doi.org/10.1007/s13399-020-00637-w

[13] Hussain, Z.A., Fakhri, F.H., Alesary, H.F. and Ahmed, L.M., 2020, November. "ZnO based material as photocatalyst for treating the textile anthraquinone derivative dye (dispersive blue 26 dye): Removal and photocatalytic treatment". In *Journal of Physics: Conference Series* (Vol. 1664, No. 1, p. 012064). IOP Publishing.. DOI 10.1088/1742-6596/1664/1/012064

[14] Karam, F.F., Saeed, N.H., Al Yasasri, A., Ahmed, L. and Saleh, H., 2020. "Kinetic study for reduced the toxicity of textile dyes (reactive yellow 14 dye and reactive green dye) using UV-A Light/ZnO system". Egyptian Journal of Chemistry, 63(8), pp.2987-2998. https://doi.org/10.21608/ejchem.2020.25893.2511

[15] Ollis, D., Silva, C.G. and Faria, J. 2015 'Simultaneous photochemical and photocatalyzed liquid phase reactions: Dye decolorization kinetics', Catalysis Today, 240, pp. 80–85. https://doi.org/10.1016/j.cattod.2014.03.062

[16] Mihsen, H.H. and Sobh, H.S. 2018. 'Preparation and characterization of thiourea-silica hybrid as heterogeneous catalyst', Asian Journal of Chemistry, 30(5). Available at: https://doi.org/10.14233/ajchem.2018.20894.

[17] Attol, D.H., Mihsen, H.H., Jaber, S.A., Alwazni, W.S. and Eesa, M.T., 2023. "Synthesis of organic functionalized silica from rice husk as an antibacterial agents". *Silicon*, *15*(5), pp.2349-2357.. https://doi.org/10.1007/s12633-022-02194-5

[18] Abbas, S.K., Hassan, Z.M., Mihsen, H.H., Eesa, M.T. and Attol, D.H., 2020. "*Uptake of Nickel (II) Ion by Silica-o-Phenylenediamine Derived from Rice Husk Ash". Silicon 12: 1103–1110* [online] https://doi.org/10.1007/s12633-019-00207-4

[19] Ridha, N.J., Alosfur, F.K.M., Kadhim, H.B.A. and Ahmed, L.M., 2021. "Synthesis of Ag decorated TiO2 nanoneedles for photocatalytic degradation of methylene blue dye". *Materials Research Express*, *8*(12), p.125013. DOI 10.1088/2053-1591/ac4408

[20] Kumar Rana, R. and Viswanathan, B. 1998. 'Mo incorporation in MCM-41 type zeolite', Catalysis Letters, 52, pp. 25–29. DOI 10.1088/2053-1591/ac4408

[21] Scimeca, M., Bischetti, S., Lamsira, H.K., Bonfiglio, R. and Bonanno, E., 2018. "Energy Dispersive X-ray (EDX) microanalysis: A powerful tool in biomedical research and diagnosis". *European journal of histochemistry: EJH*, *62*(1), p.2841. doi: 10.4081/ejh.2018.2841

[22] Chaudhary, D.S. and Jollands, M.C., 2004. "Characterization of rice hull ash". *Journal of applied*

polymer science, *93*(1), pp.1-8.. https://doi.org/10.1002/app.20217

[23] Ergün, A., 2011. "*Microwave assisted synthesis of MCM-41 type mesoporous materials and diffusion of organic vapors in porous media: MCM-41 and carbon nanotubes"* (Doctoral dissertation).

[24] Ahmed, L.M. 2018. 'Photo-decolourization kinetics of acid red 87 dye in ZnO suspension under different types of UV-A light', Asian J. Chem, 30(9), pp. 2134–2140. https://doi.org/10.14233/ajchem.2018.21520

[25] Yang, J., Zhang, J., Zhu, L., Chen, S., Zhang, Y., Tang, Y., Zhu, Y. and Li, Y., 2006. "Synthesis of nano titania particles embedded in mesoporous SBA-15: characterization and photocatalytic activity". *Journal of Hazardous Materials*, *137*(2), pp. 952- 958. https://doi.org/10.1016/j.jhazmat.2006.03.017

[26] Azeez, F , E Al-Hetlani, M Arafa, Y Abdelmonem, AA Nazeer, MO Amin, M Madkour. 2018. 'The effect of surface charge on photocatalytic degradation of methylene blue dye using chargeable titania nanoparticles', Scientific reports, 8(1), pp. 1–9. https://doi.org/10.1038/s41598-018-25673-5

[27] Kumar, D.J.V., 2016. *Determination of activation energy for encapsulant browning of photovoltaic modules*. Arizona State University.

[28] Zarrouk, A., Hammouti, B., Zarrok, H., Al-Deyab, S.S. and Messali, M., 2011. Temperature effect, activation energies and thermodynamic adsorption studies of L-cysteine methyl ester hydrochloride as copper corrosion inhibitor in nitric acid 2M. *International Journal of Electrochemical Science*, *6*(12), pp.6261-6274.. https://doi.org/10.1016/S1452-3981(23)19679-9

[29] Fu, J. 2016. "Adsorption of methylene blue by a high-efficiency adsorbent (polydopamine microspheres): kinetics, isotherm, thermodynamics and mechanism analysis," *Chem. Eng. J.*, vol. 259, pp. 53–61. https://doi.org/10.1016/j.cej.2014.07.101

[30] Kumar, D. J. V. 2016." *Determination of activation energy for encapsulant browning of photovoltaic modules*. Arizona State University.

[31] Ahmed, L.M., Tawfeeq, F.T., Al-Ameer, M.H.A., Al-Hussein, K.A. and Athaab, A.R., 2016. "Photo-degradation of Reactive Yellow 14 dye (a textile dye) employing ZnO as photocatalyst". *Journal of Geoscience and Environment Protection*, *4*(11), pp.34-44. DOI: 10.4236/gep.2016.411004

[32] Nasiri, A., Tamaddon, F., Mosslemin, M.H., Amiri Gharaghani, M. and Asadipour, A., 2019. "Magnetic nano-biocomposite $CuFe_2O_4$@ methylcellulose (MC) prepared as a new nano-photocatalyst for degradation of ciprofloxacin from aqueous solution". *Environmental health engineering and management journal*, *6*(1), pp.41-51. http://dx.doi.org/10.15171/EHEM.2019.05

[33] Tao, X. Y. 2025. "3.2 Degradation Performance of FeCoCrMoCBY Catalyst with Different Reaction Conditions in RhB," *Fe-Based Amorph. Alloy. with High Glas. Form. Abil.*, p. 266.

[34] Pitre, S.P., McTiernan, C.D. and Scaiano, J.C. 2016. 'Understanding the kinetics and spectroscopy of

photoredox catalysis and transition-metal-free alternatives', Accounts of Chemical Research, 49(6), pp. 1320–1330. https://doi.org/10.1021/acs.accounts.6b00012.